# Technical Notes

*TECHNICAL NOTES are short manuscripts describing new developments or important results of a preliminary nature. These Notes cannot exceed 6 manuscript pages and 3 figures; a page of text may be substituted for a figure and vice versa. After informal review by the editors, they may be published within a few months of the data of receipt. Style requirements are the same as for regular contributions (see inside back cover).*

## Spectral and Integrated Emittance of Ablation Chars and Carbon

R. Gale Wilson* and Cary R. Spitzer*
*NASA Langley Research Center, Hampton, Va.*

### Introduction

THE initial results of a study of the hemispherical emittance of ablation chars, carbon, and graphite from 2200 to 3450°K at wavelengths from 0.4 to 2.4 $\mu$m were presented in Ref. 1. The final results, including data at 2.8 and 3.2 $\mu$m, integrated emittance, further definition of temperature dependence, and correlation of literature data on emittance of ablation chars, are presented in this Note. In applications of the materials to atmospheric-entry heat shields, total or integrated emittance data of the type presented are necessary to determine efficiency of heat dissipation by self-radiation. The spectral data are also necessary for calculating efficiency of reflection of visible and near-infrared shock-layer radiation.

### Reflectance Measurements

Spectral emittance (absorptance) data were obtained from spectral reflectance measurements made in a double-ellipsoidal-mirror reflectometer in which a carbon arc provides incident radiation and heats the sample (Ref. 1, Fig. 1). The materials studied were phenolic-nylon chars, phenolic-carbon char, epoxy char, dense (high-purity) and porous carbon, and high-purity, structural, and pyrolytic grades of graphite. All measurements were made in air to provide some simulation of the oxidizing conditions that a heat shield experiences upon entry into the earth's atmosphere.

To make measurements possible at 2.8 and 3.2 $\mu$m, the quartz light pipes of the image pyrometer described in Ref. 1 were replaced with ones of sapphire. In general, measurements at 3.2 $\mu$m were limited to the most reflective materials under conditions of maximum incident radiation because the lead sulfide detector has a relatively low response at this wavelength.

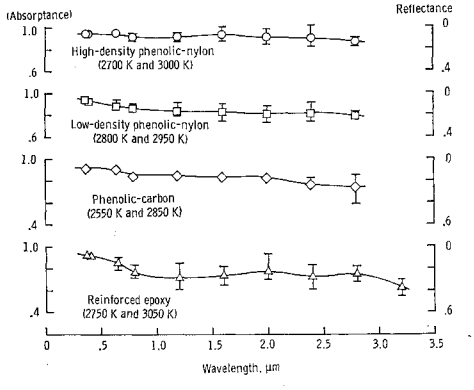


**Fig. 1 Emittance of ablation chars.**

Received January 17, 1969; revision received July 30, 1969.
* Aerospace Technologist.

Magnesium oxide prepared by the methods described in Ref. 1 served as a reflectance standard for all wavelengths. For measurements from 0.4 to 2.4 $\mu$m the MgO reflectance data of Ref. 2 were used, and data from Ref. 3 (Gier et al.) were used at 2.8 and 3.2 $\mu$m.

To obtain integrated emittance, the spectral data for each material and temperature were numerically integrated over the appropriate wavelength range. Spectral emittance values were read at wavelength increments of 0.05 $\mu$m from curves drawn through the arithmetic averages of the measured emittance values.

### Results and Discussion

The emittance and reflectance data obtained for the materials are presented as functions of wavelength and temperature in Figs. 1–3. The curves represent the averages for the measurements reported in Ref. 1 and those obtained during the final phase of the study that covered the range 0.4 to 3.2 $\mu$m. Table 1 presents the integrated emittance, the measurement temperature, the wavelength limits of integration, and the percentage of the total radiating power of a blackbody at the sample temperature that lies within the limits of the integral. The uncertainties in integrated emittance due to scatter were calculated for the curves whose data scatter appeared significantly large. Since 86–93% of the radiating power of a blackbody is accounted for in the wavelength range of the measurements for most sample temperatures, most of the integrated emittances are good approximations to total hemispherical emittance.

#### *Ablation chars*

The emittance and reflectance curves for the chars are shown in Fig. 1. The data were essentially the same for both temperatures at which each char was evaluated. In Fig. 1 the curves, from top to bottom, represent 115, 114, 54, and 71 data points, respectively. The data on low-density phenolic-nylon char represent, in addition to the two chars described in Ref. 1, a char formed from the phenolic-nylon described in Ref. 4 by a 150-sec thermal degradation in an arcjet in a flux density of 2.25 Mw/m$^2$ and a stagnation enthalpy of 37 Mjoule/kg. The emittance of low-density phenolic-nylon char was independent of the thermal degradation conditions, composition, and fabrication conditions represented.

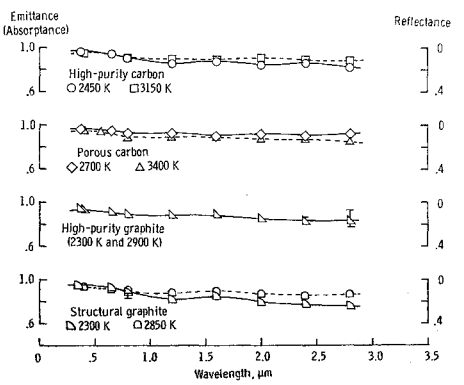


**Fig. 2 Emittance of carbon and graphite.**

**Table 1 Integrated emittance**

| Material | Temperature $T$, (°K) | Integrated emittance[a] $\epsilon$ | Wavelength range ($\mu$m) ($\lambda_1$ to $\lambda_2$) | Fraction of total blackbody power[b] between $\lambda_1$ and $\lambda_2$ |
|---|---|---|---|---|
| High-density phenolic-nylon char | 3000 | 0.91 (+0.05. −0.04) | 0.4 to 2.8 | 0.87 |
| Low-density phenolic nylon char | 2950 | 0.84 (±0.06) | 0.4 to 2.8 | 0.87 |
| Phenolic-carbon char | 2850 | 0.84 (+0.03, −0.02) | 0.4 to 2.8 | 0.86 |
| Reinforced-epoxy char | 3050 | 0.75 (+0.10, −0.08) | 0.4 to 3.2 | 0.91 |
| High-purity carbon (L113SP) | 2450 | 0.87 | 0.4 to 2.8 | 0.80 |
| | 3150 | 0.91 | 0.4 to 2.8 | 0.88 |
| Porous carbon (national grade 60) | 2700 | 0.92 | 0.4 to 2.8 | 0.84 |
| | 3400 | 0.89 | 0.4 to 2.8 | 0.90 |
| High-purity graphite (AGKSP) | 2900 | 0.88 | 0.4 to 2.8 | 0.86 |
| Structural graphite (ATJ) | 2300 | 0.82 | 0.4 to 2.8 | 0.77 |
| | 2850 | 0.86 | 0.4 to 2.8 | 0.86 |
| Pyrolytic graphite ($a$ plane) | 2200 | 0.74 | 0.4 to 2.8 | 0.75 |
| | 2850 | 0.67 | 0.4 to 3.2 | 0.89 |
| | 3300 | 0.76 (+0.10, −0.05) | 0.4 to 3.2 | 0.92 |
| Pyrolytic graphite ($c$ plane) | 2500 | 0.62 | 0.4 to 2.8 | 0.81 |
| | 2850 | 0.55 | 0.4 to 2.8 | 0.86 |
| | 3450 | 0.81 | 0.4 to 3.2 | 0.98 |

[a] $\int_{\lambda_1}^{\lambda_2} \frac{\epsilon_\lambda c_1 \lambda^{-5}}{e^{c_2/\lambda T} - 1}\, d\lambda \Big/ \int_{\lambda_1}^{\lambda_2} \frac{c_1 \lambda^{-5}}{e^{c_2/\lambda T} - 1}\, d\lambda$. [b] $\int_{\lambda_1}^{\lambda_2} \frac{c_1 \lambda^{-5}}{e^{c_2/\lambda T} - 1}\, d\lambda \Big/ \sigma T^4$.

where $c_1$, $c_2$, and $\sigma$ are radiation constants, $\epsilon_\lambda$ is the spectral emittance, and $e$ is the natural log base.

Engelke et al. have measured high-temperature total normal emittance of low-density phenolic-nylon char,[5] high-density phenolic-nylon char,[6] and phenolic-carbon char[7] of the types evaluated in the current study. Engelke used a method that assumes that the total emittance and spectral emittance are equal at 0.665 $\mu$m. If Engelke's values are corrected for this graybody-assumption error[8] by the 0.665 $\mu$m data in Fig. 1, the corrected values are within 5% of the average integrated emittance values.

The data on low-density phenolic-nylon char and the epoxy char may be compared with total normal emittance data from 1900 to 2400 K on chars of the same materials obtained by Pope.[9] The method Pope used assumes graybody behavior, also. If his 2400°K data are corrected for the graybody-assumption error on the basis of the 0.65 $\mu$m data in Fig. 1, the corrected data for the phenolic-nylon and epoxy chars are 10% and 4%, respectively, lower than the integrated emittance values. Pope's measurements were made while the samples were heated in an arcjet stream, and he points out that no account was taken of the effects of gas radiation and absorption.

Chang and Sutton[10] have reported spectral emittance data on phenolic graphite at 2500°K measured under simulated re-entry conditions at wavelengths from 0.3 to 10.5 $\mu$m. Their data agree with those obtained in this study, both in magnitude and wavelength dependence.

### *Carbon and polycrystalline graphite*

Each curve in Fig. 2 is an average curve for between 16 and 22 data points for carbon or graphite. There are some small apparent temperature dependences not recognizable in the initial study.[1]

Because of the variable factors affecting measurements, it is difficult to make comparisons of these spectral and integrated data with literature data. If appropriate comparisons are made, the results of the present study appear to be consistent with literature data and trends.[11,12]

### *Pyrolytic graphite*

The emittance data for the $a$ plane and $c$ plane of pyrolytic graphite are summarized in Figs. 3a and 3b and Table 1. Measurements were made at three temperatures for each orientation, with an average of 32 data points at each temperature for the $a$ plane and an average of 20 data points at each temperature for the $c$ plane. Definite temperature dependence for the $c$ plane emittance was established. A similar pattern of apparent temperature dependence was found for the $a$ plane emittance, but temperature dependence of emittance for this plane is not completely distinguishable from dependence on surface oxidation and erosion effects which, themselves, are time- and temperature-dependent. For example, the large scatter in the data for the $a$ plane (Fig. 3a, bottom curve) was determined to be primarily due to variations in surface conditions. Some samples after reflectance measurements had a glossy surface, whereas others had a crazed surface that apparently resulted from erosion between the crystal planes. The emittance for the crazed

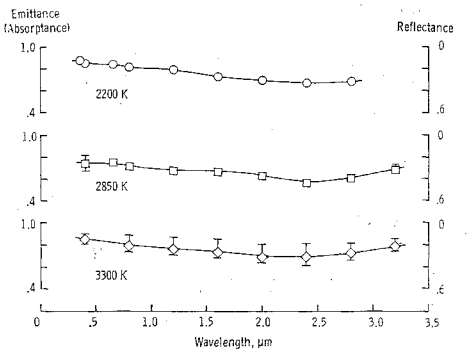


**a) *a* plane**

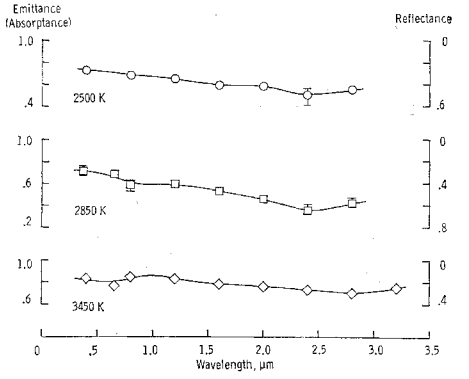


**b) *c* plane**

**Fig. 3 Emittance of pyrolytic graphite.**

surfaces was higher than that of the glossy ones, and its sensitivity to the erosive action appeared to vary from one sample to another.

The $c$ plane surface is also sensitive to oxidation, but less so than the $a$ plane surface. This surface becomes more glossy with increased temperature and exposure time. However, the highest emittance measured corresponds to the highest temperature and the most glossy surface, indicating an influence of temperature that more than compensates for surface roughness effects. Similar observations are made in Ref. 11 (p. 471). A related observation made in Ref. 13 is that surfaces etched by heating in either vacuum or argon at temperatures above 2900°K had their luster restored by heating in oxygen. The work reported in the latter reference demonstrates the sensitivity of pyrolytic graphite emittance to surface conditions and environment of heating.

### Concluding Remarks

Spectral hemispherical emittance and reflectance data have been obtained on a variety of ablation chars, carbon, and graphite at wavelengths of 0.4–3.2 $\mu$m and temperatures of 2200–3450°K. The spectral and integrated emittance data on carbon and polycrystalline graphite are in close agreement with comparable spectral and total emittance data in the literature. Total emittance data in the literature on ablation chars of the types evaluated are 10–20% lower than the integrated emittances. However, the literature data were obtained by methods based on assumed gray-body behavior of the materials, and when corrections based on the spectral definition obtained in the current study are made, the corrected values are only 2–10% lower than the integrated values.

### References


[1] Wilson, R. G. and Spitzer, C. R., "Visible and Near-Infrared Emittance of Ablation Chars and Carbon," *AIAA Journal*, Vol. 6, No. 4, April 1968, pp. 665–671.

[2] Sanders, C. L. and Middleton, W. E. K., "The Absolute Spectral Diffuse Reflectance of Magnesium Oxide in the Near Infrared," *Journal of the Optical Society of America*, Vol. 43, No. 1, Jan. 1953, p. 58.

[3] Touloukian, Y. S., ed., *Thermophysical Properties of High-Temperature Solid Materials, Vol. 4: Oxides and Their Solutions and Mixtures, Part I: Simple Oxygen Compounds and Their Mixtures*, Thermophysical Properties Research Center, Purdue Univ., 1967, p. 269.

[4] Keller, L. B., "Development of Characterized and Reproducible Syntactic Foam of Phenolic Nylon for Heat Shields," CR-73041, 1965, NASA.

[5] Engelke, W. T., Pyron, C. M., and Pears, C. D., "Thermophysical Properties of a Low-Density Phenolic-Nylon Ablation Material," CR-809, July 1967, NASA.

[6] Wilson, R. G., compiler, "Thermophysical Properties of Six Charring Ablators from 140 to 700 K and Two Chars from 800 to 3000 K," TN D-2991, Oct. 1965, NASA.

[7] Engelke, W. T., Pyron, C. M., and Pears, C. D., "Thermal and Mechanical Properties of a Nondegraded and Thermally Degraded Phenolic-Carbon Composite," CR-896, Oct. 1967, NASA.

[8] Evans, R. J., Clayton, W. A., and Fries, M., "A Very Rapid 3000°F Technique for Measuring Emittance of Opaque Solid Materials," *Measurement of Thermal Radiation Properties of Solids*, edited by J. C. Richmond, NASA SP-31, 1963, pp. 483–488.

[9] Pope, Ronald B., "Measurements of the Total Surface Emittance of Charring Ablators," *AIAA Journal*, Vol. 5, No. 12, Dec. 1967, pp. 2285–2287.

[10] Chang, J. H. and Sutton, G. W., "Spectral Emissivity Measurements of Ablating Phenolic Graphite," *AIAA Journal*, Vol. 7, No. 6, June 1969, pp. 1110–1114.

[11] Plunkett, J. D. and Kingery, W. D., "The Spectral and Integrated Emissivity of Carbon and Graphite," *Proceedings of the Fourth Conference on Carbon*, Pergamon, New York, 1960, pp. 457–472.

[12] Grevis, A. F. and Levitt, A. P., "The Spectral Emissivity and Total Normal Emissivity of Commercial Graphites at Elevated Temperatures," *Proceedings of the Fifth Conference on Carbon*, Vol. 2, Pergamon, New York, 1963, pp. 639–646.

[13] Champetier, Robert J., "Basal Plane Emittance of Pyrolytic Graphite at Elevated Temperatures," Air Force Rept. SAMSO-TR-67-5, Aerospace Rept. TR-0158(3250-20)-10, July 1967, The Aerospace Corp.


# Uncertainties of Calculated Characteristics of a Transpiration-Cooled Arc


Ekkehard Marschall*
*University of Minnesota, Minneapolis, Minn.*


### Nomenclature

$c_p$ = specific heat at constant pressure
$E$ = electric field strength
$h$ = enthalpy
$H$ = mass average enthalpy
$I$ = electric current
$k$ = thermal conductivity
$\dot{m}$ = mass injection rate through porous wall
$p$ = pressure
$P_r$ = heat loss by radiation
$r,z$ = coordinates
$T$ = temperature
$v$ = velocity
$\dot{w}$ = mass flow within constrictor in $z$ direction
$\mu$ = viscosity
$\mu_0$ = susceptibility of vacuum
$\zeta$ = bulk viscosity
$\rho$ = gas density
$\sigma$ = electrical conductivity

***Subscripts***

0 = on axis
$p$ = in plenum chamber around outside wall
$w$ = at constrictor wall

FOR the generation of a high-temperature, high-density plasma, transpiration-cooling of the constrictor tube in which the electric arc is operated has been suggested and corresponding experiments in this laboratory are already in progress.[1,2] From theoretical considerations, it seems possible to achieve higher axis temperatures with such an arc than with the conventional water-cooled cascaded arc.

In this work, the uncertainty of theoretical predictions, which suffer mainly from uncertainties of published values of the plasma transport properties, will be analyzed. The results of this study may be useful for other investigations as well which rely on the knowledge of the thermodynamic and transport properties of high-temperature plasmas.

Recently, Anderson described a method for the calculation of the characteristics of a transpiration-cooled arc[3] based on some earlier work of Anderson and Eckert.[4] In connection with analyzing the performance capability of a transpiration-cooled constricted arc heater, Anderson and Eckert used this method successfully.[5] Assuming a thermally and hydrodynamically fully developed laminar flow, the continuity,

Received March 4, 1968; revision received January 9, 1969.

* NATO-Scholar, Heat Transfer Laboratory, School of Mechanical and Aerospace Engineering; now Assistant Professor, Department of Mechanical Engineering, University of California, Santa Barbara, Calif.